


Semi-Mechanistic PK/PD Modeling and Simulation of Irreversible BTK Inhibition to Support Dose Selection of Tirabrutinib in Subjects with RA

Amy Meng^{1,*}, Rita Humeniuk¹, Juliane M. Jürgensmeier¹, Chia-Hsiang Hsueh¹, Franziska Matzkies¹, Ethan Grant¹, Hoa Truong¹, Andrew N. Billin¹ , Helen Yu¹, Joy Feng¹, Ellen Kwan¹, Thomas Tarnowski¹ and Cara H. Nelson¹

Tirabrutinib is an irreversible, small-molecule Bruton's tyrosine kinase (BTK) inhibitor, which was approved in Japan (VELEXBRU) to treat B-cell malignancies and is in clinical development for inflammatory diseases. As an application of model-informed drug development, a semimechanistic pharmacokinetic/pharmacodynamic (PK/PD) model for irreversible BTK inhibition of tirabrutinib was developed to support dose selection in clinical development, based on clinical PK and BTK occupancy data from two phase I studies with a wide range of PK exposures in healthy volunteers and in subjects with rheumatoid arthritis. The developed model adequately described and predicted the PK and PD data. Overall, the model-based simulation supported a total daily dose of at least 40 mg, either q.d. or b.i.d., with adequate BTK occupancy (> 90%) for further development in inflammatory diseases. Following the PK/PD modeling and simulation, the relationship between model-predicted BTK occupancy and preliminary clinical efficacy data was also explored and a positive trend was identified between the increasing time above adequate BTK occupancy and better efficacy in treatment for RA by linear regression.

Study Highlights

WHAT IS THE CURRENT KNOWLEDGE ON THE TOPIC?

✓ Tirabrutinib is an irreversible, small molecule Bruton's tyrosine kinase (BTK) inhibitor, which was approved in Japan (VELEXBRU) to treat B-cell malignancies and is in clinical development for inflammatory diseases.

WHAT QUESTION DID THIS STUDY ADDRESS?

✓ A semimechanistic pharmacokinetic/pharmacodynamic (PK/PD) model for irreversible BTK inhibition of tirabrutinib was developed to support dose selection in clinical development, based on clinical PK and BTK occupancy data from two phase I studies.

WHAT DOES THIS STUDY ADD TO OUR KNOWLEDGE?

✓ The developed model adequately described and predicted the PK and PD data. Overall, the model-based simulation

supported a dosing regimen of a total daily dose of at least 40 mg with adequate BTK occupancy for further development. In addition, a positive trend was identified between the increasing time above adequate BTK occupancy and better efficacy in treatment of rheumatoid arthritis.

HOW MIGHT THIS CHANGE CLINICAL PHARMACOLOGY OR TRANSLATIONAL SCIENCE?

✓ Quantitative pharmacology tools can be utilized in early phase trials to bridge nonclinical data to clinical data to select a dosing regimen for BTK inhibitors for further evaluation.

Bruton's tyrosine kinase (BTK) plays key roles in the pathogenesis of many B-cell malignancies and inflammatory diseases through B-cell development and activation via the B-cell receptor (BCR) signaling.¹⁻⁴ BTK inhibition as a target has been demonstrated to provide a clinical benefit in different types of B-cell malignancies,

as supported by the clinical data of covalent irreversible BTK inhibitors, including ibrutinib, acalabrutinib, zanubrutinib, and tirabrutinib (GS-4059 and ONO-4059), which were all granted marketing approval for treatment of B-cell malignancies.⁵⁻⁸ Given the central role of BTK in immune cell signaling, inhibition of

¹Gilead Sciences, Inc., Foster City, California, USA. *Correspondence: Amy Meng (amy.meng@gilead.com)

Received June 9, 2021; accepted September 14, 2021. doi:10.1002/cpt.2439

BTK is also expected to have pleiotropic anti-inflammatory effects and to affect multiple steps in the pathogenesis of inflammatory diseases, including rheumatoid arthritis (RA). In preclinical models, BTK inhibition suppresses BCR-stimulated proliferation, costimulatory molecule expression, and autoantibody production in B cells.^{9–12} Clinical data showed that fenebrutinib, a reversible BTK inhibitor, has demonstrated efficacy comparable with adalimumab in patients with moderate-to-severe RA¹³; spebrutinib, which is an irreversible BTK inhibitor, has been found to reduce disease markers in patients with active RA.¹⁴ These encouraging results prompted a search for more BTK inhibitors for the treatment of RA with a favorable risk/benefit profile, especially among the well-studied and approved BTK inhibitors.

Tirabrutinib, a highly potent, selective, and irreversible small molecule that blocks BTK autophosphorylation, was approved in Japan (VELEXBRU) to treat B-cell malignancies, including relapsed or refractory primary central nervous system lymphoma, Waldenström macroglobulinemia, and lymphoplasmacytic lymphoma, and is in clinical development for inflammatory diseases.^{6–8,15–18} In previous preclinical studies, tirabrutinib has shown to prevent the production of inflammatory mediators in monocytes, mast cells, and osteoclasts, and has demonstrated a dose-dependent inhibition of arthritis severity and bone damage in the murine collagen-induced arthritis model.¹⁹ In a phase I dose escalation study, tirabrutinib was rapidly absorbed following oral administration and exhibited dose-proportional pharmacokinetics (PKs) over a 20-to-320 mg dose range.²⁰ Tirabrutinib was generally well-tolerated in patients with evaluated B-cell malignancies, with an acceptable safety profile for doses ranging from 20 to 480 mg once daily (q.d.).^{6,8,16,17,20}

This article describes the use of a semimechanistic PK/pharmacodynamic (PD) model to guide dose selection of tirabrutinib for future clinical studies in inflammatory diseases by using the pooled data from the two phase I studies of tirabrutinib. The model prediction was further applied to deconvolute the linkage between BTK occupancy and treatment effect.

METHODS

Study design

Study protocols for the two phase I studies were approved by an independent review board prior to study initiation, and all subjects provided written informed consent before participating. The studies were conducted in accordance with ethical principles originating in the Declaration of Helsinki and in compliance with Good Clinical Practice guidelines and applicable regulatory laws. Study design of the two studies is summarized in **Table 1**.

Subjects

Key inclusion and exclusion criteria were the same for healthy subjects in both phase I studies. Male and female subjects aged 18–45 years were eligible if they had a body mass index of 19–30 kg/m², were non-smokers, had creatinine clearance \geq 90 mL/min using the Cockcroft-Gault method,²¹ and had laboratory parameters within the normal range of the testing laboratory. For part B in study #2, male and female subjects aged 18–65 years with a diagnosis of RA were eligible if they had stable ongoing treatment of methotrexate and folic or folinic acid supplement and had creatinine clearance \geq 60 mL/min (Cockcroft-Gault method). Active RA was not a requirement to participate in part B, study 2. Additional exclusion criteria are listed in **Supplementary Materials**.

Pharmacokinetics

Details of PK sampling for the two studies are outlined in **Supplementary Figure S3**. Plasma tirabrutinib concentrations were determined using a validated high-performance liquid chromatography-tandem mass spectrometry (LC-MS/MS) method with isotopically labeled tirabrutinib as internal standard and a lower limit of quantitation (LLOQ) of 1.0 ng/mL. All the concentrations were measured by using the same LC-MS/MS method in the same center at Syneos, Princeton, NJ, USA.

Pharmacodynamics

BTK occupancy, which is the PDs in both studies, were evaluated using the BTK occupancy test, which is performed in peripheral blood mononuclear cells and is a duplexed, homogeneous, time-resolved fluorescence resonance energy transfer assay that measures total and free BTK in the same well. Details of the methods have been published previously.²² In Study #1, samples collected on day 1 for evaluation in the BTK occupancy assay were not evaluable due to low cell viability;

Table 1 Study design summary in each of the two phase I studies

	Study 1 (healthy volunteers) ^a	Study 2 (healthy volunteers) Part A	Study 2 (patients with RA) ^b Part B
Objective	<ul style="list-style-type: none"> To evaluate the effect of OATP 1B1/1B3 inhibition (using single-dose rifampin) and CYP3A/P-gp induction (using multiple-dose rifampin) on the PKs of tirabrutinib To evaluate BTK target inhibition,^{22,29} based on preclinical DDI data³⁰ 	<p>To evaluate the safety of tirabrutinib in healthy volunteers and in subjects with RA (primary)</p> <p>To evaluate PK and PD of tirabrutinib in healthy subjects (secondary)</p>	To evaluate tirabrutinib effect on disease-specific clinical markers and outcomes in subjects with RA (secondary)
Subjects	15 healthy male and nonpregnant, nonlactating female subjects, 18 to 45 years of age (inclusive)	Healthy male and nonpregnant, nonlactating female subjects 18 to 45 years of age, inclusive	20 subjects with RA
Treatment	Tirabrutinib 100 mg on day 1; tirabrutinib 100 mg plus rifampin 600 mg coadministered on day 8; rifampin 600 mg q.d. for 7 days (days 10–16); and tirabrutinib 100 mg on day 17	Randomized 4:1 in a blinded fashion to receive tirabrutinib 20 mg or placebo orally q.d. (cohort 1) or tirabrutinib 10 mg or placebo orally b.i.d. (cohort 2) for 1 week in each cohort	Randomized 4:1 in a blinded fashion to receive tirabrutinib 20 mg q.d. or placebo q.d. for 4 weeks and were then followed for 4 weeks following treatment completion

BTK, Bruton's tyrosine kinase; DDI, drug-drug interaction; PD, pharmacodynamic; PK, pharmacokinetic; RA, rheumatoid arthritis;

^aAdditional study design details for study 1 are in **Supplementary Figure S1**. ^bAdditional study design details for part B, study 2 (NCT02626026) are in **Supplementary Figure S2**.

therefore, interpretation of data in study #1 was restricted to days 8 and 17, using the predose samples on day 8 as baseline. Details of definition of the lower limit of detection and imputation practices are available in **Supplementary Figure S4**. In study #2, for both cohorts in part A, total and free BTK were collected at baseline, on days 1, 2, 3, 5, and 7, and up to postdose 120 hours after the last dose. In cohort 2, baseline samples were not considered evaluable. In part B, total and free BTK were collected at the baseline and the postdose timepoints when PK samples were collected (**Supplementary Figure S3**). A subject was excluded from the analysis set if total BTK was less than the LLOQ (i.e., 12 ng/mL) or free BTK less than the LLOQ (i.e., 12 ng/mL) at baseline. A sample for a given visit was excluded from the analysis set if total BTK less than the LLOQ (i.e., 12 ng/mL).

Efficacy in study #2, part B

Efficacy end points included the American College of Rheumatology (ACR) core data set variables and high-sensitivity C-reactive protein (hsCRP) plasma concentration and tender joint count 68 (TJC68) were further evaluated on PD-efficacy relationships.

PK/PD modeling and simulation

In the PK/PD model, a two-compartment PK model with a first-order absorption, including lag time was used to fit the PK data, parameterized in terms of apparent clearance (CL/F), apparent central volume of distribution (V_c/F), apparent intercompartmental clearance, apparent peripheral volume of distribution, absorption rate constant (k_a), absorption lag time, and relative bioavailability. Interindividual variability (IIV) was included on CL/F, V_c/F , and k_a . Following the development of the PK model, the PK/PD model was subsequently developed based on individual estimates from the PK model. For the modeling of target occupancy, a mechanism (**Scheme 1**) was considered in which there is a reversible, pre-equilibrium binding of inhibitor (I) to enzyme (E) characterized by the binding constant K_i , and an irreversible, covalent modification step described by the first-order rate constant k_{inact} . The ratio k_{inact}/K_i has the form of a second-order rate constant and was obtained in *in vitro* binding experiments.¹⁸

A covalent binding model was used to describe target occupancy by tirabrutinib and free BTK level. Because a higher total BTK level was observed after multiple dosing of tirabrutinib compared to day 1, which may be due to greater BTK synthesis rate stimulated by BTK inhibition, a negative feedback mechanism on BTK synthesis was incorporated into the PK/PD model. Equations 1 and 2 were used for predicting free BTK and total BTK, respectively, where fBTK = free BTK level, tBTK = total BTK level, $b/fBTK$ = baseline free BTK, $k_{in-free}$ = free protein (BTK) production rate, $k_{in-total}$ = total protein (BTK) production rate, k_{syn} = feedback rate constant on protein synthesis from BTK inhibition, f_u = fraction unbound of tirabrutinib, C_{tira} = plasma concentration of tirabrutinib, and $kdeg$ = protein degradation rate (same rate was assumed for both free BTK and bound BTK). The $k_{in-total}$ was parameterized to account for binding to endogenous ligands and existing concomitant medication. IIV was included on fBTK and tBTK in the PD model.

$$dfBTK/dt = k_{in-free} - k_{inact}/K_i \times fBTK \times f_u \times C_{tira} - fBTK \times kdeg \quad (1)$$

$$dtBTK/dt = k_{in-total} \times (fBTK/bfBTK)^{k_{syn}} - tBTK \times kdeg \quad (2)$$

The Non-Linear Mixed Effect Modeling (NONMEM) program (NONMEM 7, version 7.4.3; ICON Development Solutions, Ellicott City, MD, USA) and PerlSpeaksNONMEM version 4.8.1 (Uppsala University, Sweden) were used for population PK and PD analysis.^{23–26} R software version 3.3.2 was used for data postprocessing and visualization. In this analysis, population mean parameters and variability—including

IIV and residual errors—are estimated, with minimization of the objective function value (OFV; $-2 \log$ likelihood ($-2LL$)) and the use of first-order conditional estimation with interaction method in NONMEM.

Model development was performed to optimize: (i) structural PK/PD model (including IIV assessment), (ii) residual error model, and (iii) covariate selection. Both decrease in OFV and diagnostic plots were used for model evaluation. Finally, bootstrap resampling techniques were used to evaluate the model stability and confidence interval (CI) of final parameter estimates.²⁷

In the covariate analysis, body weight, age, gender, race, ethnicity, body surface area, baseline alanine aminotransferase, baseline aspartate aminotransferase, and baseline albumin were tested as covariates on CL/F, V_c/F , and k_a in the PK model. RA disease status (subjects with RA vs. healthy subjects) was tested on fBTK and tBTK in the PD model. A stepwise forward addition ($\Delta OFV > 6.64$, $P < 0.01$) and backward deletion ($\Delta OFV > 10.83$, $P < 0.001$) strategy was used to identify covariate effects yielding statistically significant decrease in $-2LL$ function in the model development.

Simulation was performed based on the final PK/PD model with virtual subjects $N = 1000$ for dosing regimens of interest. The evaluated dosing regimens included 10, 20, 40, 80, and 160 mg q.d. dose; and 10, 20, and 40 mg b.i.d. dose. BTK inhibition was targeted at 90%, which was achieved by the efficacious doses of BTK inhibitor fenebrutinib in subjects with RA.^{13,28}

Statistics

In study #2, efficacy data were collected in part B and the PD-efficacy relationship was further explored in subjects with RA by using model-predicted individual target occupancy and the evaluated efficacy end points (hsCRP and TJC68) by using linear regression. Efficacy assessments were performed at study visits on day 1 (predose), week 2, and week 4 visits.

RESULTS

Subject Demographics

Demographics for the subjects enrolled in each of the two phase I studies are summarized in **Table 2**.

PK of tirabrutinib

The PK profiles of tirabrutinib are presented for study #1 (**Figure AS1**) and for study #2 (**Figure AS2** and **Figure AS3**). A biphasic PK profile was shown with median half-life ranging from ~ 6.2 to ~ 7.3 hours. Accumulations demonstrated with plasma concentrations for multiple doses were generally higher compared with those following a single dose.

Free BTK after administration of tirabrutinib

Normalized free BTK after tirabrutinib administration is shown for study #1 (**Figure BS1**) and for study #2 (**Figure BS2** and **Figure BS3**). Normalized fBTK levels decreased rapidly after tirabrutinib administration. Recovery of BTK levels was slower compared to the rapid decline in plasma concentrations. The half-life of BTK and prolonged PD effect was dissociated with remaining tirabrutinib concentrations, as expected with an irreversible inhibitor.



Scheme 1 Reaction scheme for irreversible inhibition.

Table 2 Demographics for subjects enrolled in each of the two phase I studies

	Study 2 (healthy volunteers) Part A: Cohort 1		Study 2 (healthy volunteers) Part A: Cohort 2		Study 2 (patients with RA) Part B	
	Tirabrutinib 20 mg q.d. N = 8	Placebo N = 2	Tirabrutinib 20 mg q.d. N = 8	Placebo N = 1 ^b	Tirabrutinib N = 16	Placebo N = 5
Age, years median (range)	33 (18–41)	37 (29–44)	36 (22–45)	43	58 (38–64)	54 (35–64)
Sex, n (%) (female)	6 (40%)	1 (50)	2 (25)	0	13 (81.3)	4 (80.0)
Race, n (%)						
Black or African American	4 (50)	0	0	1	0	0
Native Hawaiian or Other Pacific Islander	0	0	0	0	0	0
White	4 (50)	2 (100)	8 (100)		16 (100)	5 (100)
Ethnicity, n (%)						
Hispanic or Latino	8 (100)	2 (100)	8 (100)	1	2 (12.5)	2 (40)
Not Hispanic or Latino	0	0	0	0	14 (87.5)	3 (60)
BMI (kg/m ²)						
Mean (SD)	26.0 (2.49)	26.7 (0.85)	27.2 (3.0)	28.4	30.2 (6.24)	39.5 (12.5)
Median (Q1, Q3)	26.0 (24.6, 28.2)	26.7 (26.1, 27.3)	28.8 (25.1, 29.3)		28.7 (25.1, 35.8)	38.3 (37.7, 38.4)
Min/Max	20.3, 29.4	26.1, 27.3	21.7, 29.8		23.0, 41.8	23.9, 58.9
Creatinine clearance ^a (mL/min)						
Mean (SD)	118.04 (14.31)	133.30 (2.70)	138.64 (18.85)		109.23 (28.15)	163.03 (36.55)
Median (Q1, Q3)	116.13 (105.1, 126.4)	133.30 (130.6, 136.0)	141.25 (128.2, 162.4)	100.37	96.95 (86.3, 127.6)	153.77 (149.0, 177.6)
Min, Max	99.6, 149.2	130.6, 136.0	109.0, 164.6		72.3, 167.6	96.3, 215.6
ALT						
Mean (SD)	15.5 (7.38)	17.0 (2.00)	20.9 (6.75)	17.0	19.0 (8.28)	23.6 (8.38)
Median (Q1, Q3)	13.0 (9.00, 21.0)	17.0 (15.0, 19.0)	19.0 (17.0, 29.0)		16.0 (13.0, 24.0)	20.0 (18.0, 24.0)
Min, Max	7.00, 36.0	15.00, 19.0	9.00, 30.0		9.00, 43.0	17.0, 39.0
AST						
Mean (SD)	17.6 (5.05)	16.5 (3.51)	18.6 (3.27)	17.0	20.3 (4.12)	19.1 (4.15)
Median (Q1, Q3)	15.0 (14.0, 21.0)	16.5 (13.0, 20.0)	18.0 (16.0, 23.0)		20.0 (18.0, 23.0)	18.0 (17.0, 20.0)
Min, Max	13.0, 32.0	13.0, 20.0	15.0, 24.0		14.0, 30.0	14.0, 26.0
Albumin						
Mean (SD)	4.30 (0.24)	4.25 (0.15)	4.57 (0.24)	4.60	4.27 (0.24)	4.16 (0.20)
Median (Q1, Q3)	4.30 (4.20, 4.50)	4.25 (4.10, 4.40)	4.60 (4.20, 4.70)		4.30 (4.20, 4.40)	4.20 (3.90, 4.30)
Min, Max	3.80, 4.80	4.10, 5.00	4.20, 4.90		3.60, 4.90	3.90, 4.40
BSA						
Mean (SD)	1.87 (0.14)	1.87 (0.29)	1.95 (0.16)	1.83	1.90 (0.19)	2.19 (0.24)
Median (Q1, Q3)	1.86 (1.72, 1.97)	1.87 (1.59, 2.16)	2.00 (1.91, 2.05)		1.91 (1.72, 2.03)	2.30 (2.07, 2.35)
Min, Max	1.67, 2.11	1.59, 2.16	1.63, 2.17		1.54, 2.20	1.65, 2.37

All the subjects who had evaluated PK and PD data in the analysis dataset were included in this table.

ALT, alanine aminotransferase; AST, aspartate aminotransferase; BMI, body mass index; BSA, bovine serum albumin; PD, pharmacodynamic(s); PK, pharmacokinetic(s); Q1, quartile 1; Q3, quartile 3; QD, once daily; RA, rheumatoid arthritis; SD, standard deviation.

^aCockcroft-Gault Method. ^bTwo subjects were enrolled and only one subject had evaluable PK and PD data in the dataset.

Summary of efficacy results from part B in study #2

For part B of study #2, various efficacy end points, including hsCRP and TJC68, were evaluated in subjects diagnosed with RA after treatment of tirabrutinib at 20 mg q.d. At the week 4 visit, subjects in the tirabrutinib group experienced a small numerical decrease in hsCRP levels and TJC68, and subjects in the placebo group experienced a small numerical increase or no change; efficacy data at week 2 were inconsistent between the two end points. The week 4 observations were maintained after stopping treatment. Because study #2 was designed to evaluate the safety, PK, and PD of tirabrutinib, and active disease was not required for enrollment, efficacy results from study #2 were exploratory and should be interpreted with caution.

PK/PD modeling and simulation

The original PK/PD dataset contained 659 tirabrutinib concentration-time datapoints, 249 fBTK and 249 tBTK datapoints in 15 subjects from study #1; and 676 concentration-time datapoints, 706 fBTK and 706 tBTK datapoints in 40 subjects from study #2. Among these samples, 232 below the limit of quantification (BLOQ) PK samples were not included and 138 PD samples were excluded due to the reasons described in the Methods section above in the analysis. The remaining data in the Model Development Dataset had 1103 PK datapoints and 1771 PD datapoints from 55 subjects.

Tirabrutinib plasma concentrations from pooled data of the two studies were best described by a two-compartment model, including a first-order absorption with lag time, with IIV on CL/F , V_c/F , and k_a . Consistent with results from intensive PK analysis,

the relative bioavailability of tirabrutinib was estimated to decrease by 72% after administration of multiple doses of rifampin (a strong CYP3A4 and P-gp inducer). The only other significant covariate in the final PK model was age on k_a . The M3 method was tested and resulted in similar parameter estimates but a worse model fit compared to the final model without the M3 method.

Following the PK model development, the PK/PD model was subsequently developed based on individual estimates from the PK model. As described in Methods above, indirect response models were used to describe both free and total BTK level, with IIV on baseline fBTK and tBTK. For the fBTK model, first-order irreversible covalent binding was modeled to describe target engagement by tirabrutinib. In the tBTK model, a negative feedback mechanism on BTK synthesis was incorporated to describe the small fluctuation observed in tBTK level over time. The only significant covariate in the PK/PD model was disease status (healthy vs. RA) on baseline fBTK. Subjects with RA showed lower levels of fBTK at baseline compared with healthy subjects with typical value of 16 ng/mL in subjects with RA and 58 ng/mL in healthy subjects and 49.2% IIV.

Consistent with the observed fBTK, the model showed that fBTK levels decreased rapidly after tirabrutinib administration and the BTK suppression was maintained through a 24-hour dosing interval after multiple dosing of tirabrutinib (**Figure 1**). The change in tBTK over time was minimal though, as was shown in visual predictive check (VPC; **Figure 1**).

Overall, the final PK/PD model adequately described the central tendency and variability in the observed PD data based on VPC, goodness-of-fit, and normalized prediction distribution

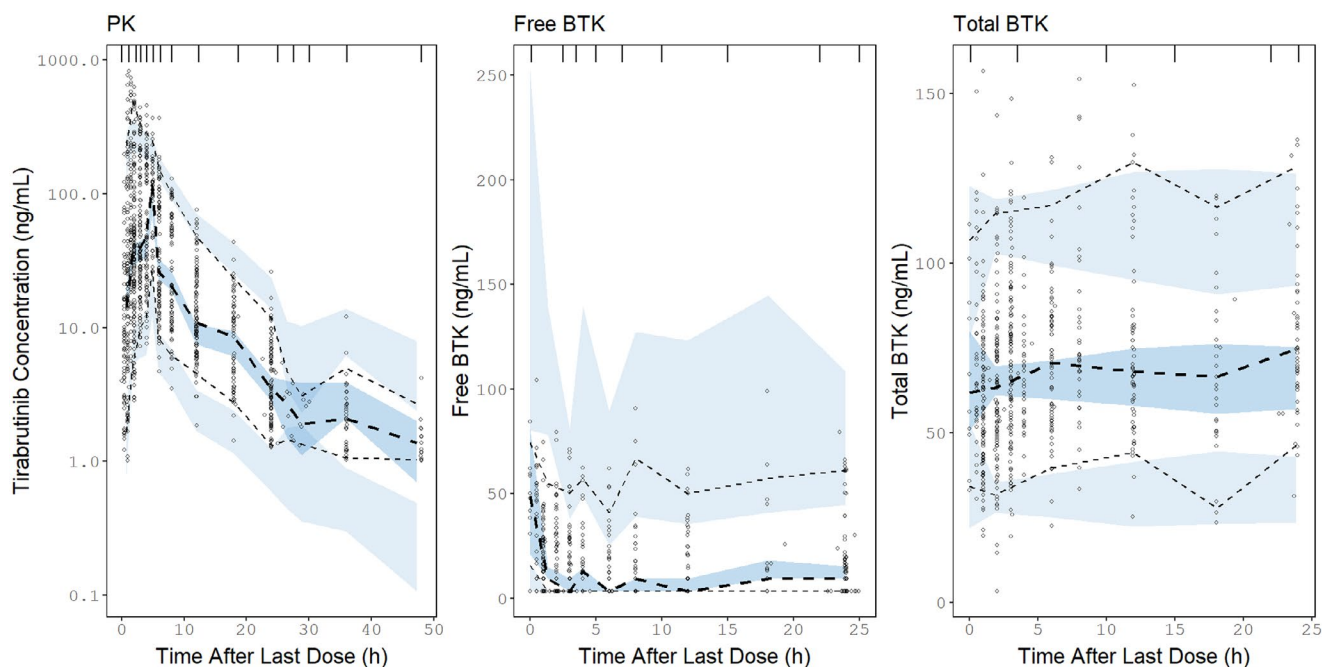


Figure 1 Visual predictive check for plasma concentrations, free BTK, and total BTK in the final PK/PD model based on pooled data from two studies. VPC plots show the median (bold dashed line) and spread (5th to 95th percentile; fine dashed lines) of the observed concentrations in all subjects. The darker blue area is the 95% CI of the simulated median, and the lighter blue area is the 95% CI of the simulated 5th and 95th percentiles. The solid blue line is the simulated median. Open circles show the observed data. BTK, Bruton's tyrosine kinase; CI, confidence interval; PD, pharmacodynamic(s); PK, pharmacokinetic(s); VPC, visual predicted check. [Colour figure can be viewed at wileyonlinelibrary.com]

Table 3 Model parameters of the final PK/PD model and parameter precision from bootstrap (N = 1000)

Parameter	Parameter description	Final PopPK model estimates (RSE%)	Bootstrap final model median estimates	Bootstrap final model	
				2.5th Percentile	97.5th Percentile
PK Parameters					
θ_1	Apparent oral clearance, CL/F (L/h)	62.6 (4)	62.5	57.4	68.5
θ_2	Apparent oral volume, V_c/F (L)	357 (7)	357	300	414
θ_3	Apparent intercompartmental clearance, Q/F (L/h)	13.4 (24)	13.8	8.76	21.9
θ_4	Apparent peripheral volume of distribution of the drug V_p/F , (L)	123 (13)	123	90.9	167
θ_5	Absorption rate constant, k_a (h^{-1})	0.800 (14)	0.811	0.620	1.11
θ_6	Absorption lag time (h)	0.465 (1)	0.465	0.454	0.474
$\sqrt{\theta_7}$	Residual error for plasma concentration (%)	60.0 (4)	59.7	57.0	62.6
θ_8	Relative bioavailability after multiple doses of rifampin	0.285 (7)	0.284	0.247	0.325
θ_9	Influence of age on k_a	-1.74 (26)	-1.74	-2.78	-0.796
ω_{CL}^2	IIV of CL/F (%)	27.5 (7)	27.1	22.3	31.0
ω_{VC}^2	IIV of V_c/F (%)	53.7 (10)	53.7	40.3	63.4
ω^{2ka}	IIV of k_a (%)	93.4 (13)	89.6	63.9	114
$\omega_{CovCLVc}^2$	Covariance between CL/F and V_c/F	0.111 (23)	0.106	0.053	0.156
PD parameters					
θ_1	Baseline free BTK for healthy subjects, fBTK (ng/mL)	58.4 (6)	58.4	51.0	67.1
θ_2	BTK turnover rate, kdeg (h^{-1})	FIX to 0.0289 ³¹			
θ_3	Covalent binding rate, kinact/Ki ($M^{-1} s^{-1}$)	FIX to $2.4 * 10^{418}$			
θ_4	Baseline total BTK, tBTK (ng/mL)	65.8 (3)	65.7	61.0	70.5
θ_5	Feedback rate constant on protein synthesis from BTK inhibition, ksyn (h^{-1})	-0.0301 (59)	-0.0290	-0.069	0.00765
$\sqrt{\theta_6}$	Residual error on free BTK for healthy subjects (%)	86.3 (8)	86.5	79.6	93.6
θ_7	Baseline free BTK for subjects with RA (ng/mL)	16.1 (6)	16.0	13.2	19.3
$\sqrt{\theta_8}$	Residual error on total BTK (%)	53.4 (5)	53.3	51.0	56.3
$\sqrt{\theta_9}$	Residual error on free BTK for subjects with RA (%)	74.1 (8)	73.9	67.5	79.9
ω_{fBTK}^2	IIV of fBTK (%)	49.2 (9)	48.0	39.3	56.8
ω_{tBTK}^2	IIV of tBTK (%)	22.1 (9)	21.7	17.9	25.8
$\omega_{CovfBTK,tBTK}^2$	Covariance between fBTK and tBTK	0.0203 (72.4)	0.0195	-0.0138	0.0495

BTK, Bruton's tyrosine kinase; CL/F, apparent clearance; fBTK, free BTK; h, hour; IIV, interindividual variability; k_a , absorption rate constant; Ki, enzymatic binding constant; kinact, covalent inactivation rate constant; PD, pharmacodynamic(s); PK, pharmacokinetic(s); PopPK, population PK; QF, apparent inter-compartmental clearance; RA, rheumatoid arthritis; RSE, relative standard error; tBTK, total BTK; V_c/F , apparent control volume of distribution; V_p/F , apparent peripheral volume of distribution.

error (NPDE; **Figure 1**, **Figures S4–S6**) and the model parameters were estimated with reasonable precision from bootstrap ($N = 1000$; **Table 3**). The shrinkage values for IIV are all below 20%. Thus, the model could be used for subsequent simulation to support dose selection for further development.

Based on the final PK/PD model, simulations were conducted to illustrate the achievable and calculated level of BTK occupancy (0–100%) for a wide range of doses being considered for further development (**Figure 2**). For q.d. dosing, the simulations showed that doses of 40 mg and above are highly overlapped across the

5%–95% prediction intervals of simulated BTK occupancy, and there is a separation between ≥ 40 mg and lower doses regarding target coverage. A dose of 40 mg q.d. at steady-state can achieve 95% BTK occupancy over the dosing interval for a typical subject and 90% of the simulated population can maintain > 90% occupancy during most of the dosing interval, which is considered adequate based on the prespecified criteria. For b.i.d. dosing, 10, 20, and 40 mg b.i.d. doses all cover 95% BTK occupancy over the dosing interval for a typical subject, and 90% of the simulated population can maintain > 90% occupancy for all the evaluated b.i.d.

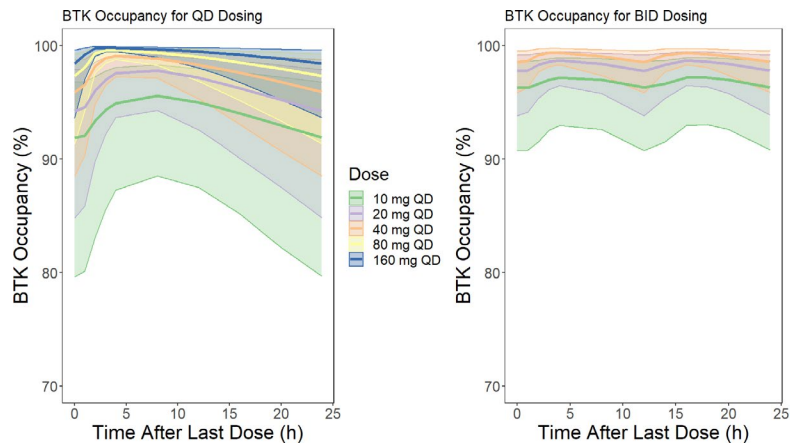


Figure 2 Model-based simulated BTK occupancy (%) for evaluated doses over a 24-hour dosing interval at steady-state after multiple dosing of tirabrutinib. The simulation plots show the median (bold solid line) and spread (5–95% prediction interval; fine solid lines) of simulated BTK occupancy with $N = 1000$. Different colors in lines and spread represent different dosing regimens of interest. The 100 on the y-axis represents full target occupancy (100%) and 70 represents 70% target occupancy. BID twice daily; BTK, Bruton's tyrosine kinase; QD, once daily. [Colour figure can be viewed at wileyonlinelibrary.com]

doses. Overall, a total daily dose of ≥ 40 mg, either q.d. or b.i.d., can achieve adequate and similar BTK occupancy across the evaluated doses.

PD-efficacy analysis

In study #2, the PD-efficacy relationship was explored in subjects with RA ($N = 21$) by using model-predicted target occupancy and exploratory efficacy end points, including hsCRP and TJC68. Efficacy assessments were performed at day 1 (predose), week 2,

and week 4 study visits. Based on the exploratory efficacy analysis, tirabrutinib had modest effects on disease-related outcomes.

Linear regressions were performed to explore the relationships between time above 90% BTK occupancy during a 24-hour dosing interval (24 hours) and efficacy end points, including hsCRP and TJC68. The regressions on hsCRP at week 2 and TJC68 at week 4 show statistically significant association ($P < 0.05$) with time above 90% BTK occupancy, whereas test on hsCRP at week 4 and TJC68 at week 2 only shows the same trend without the

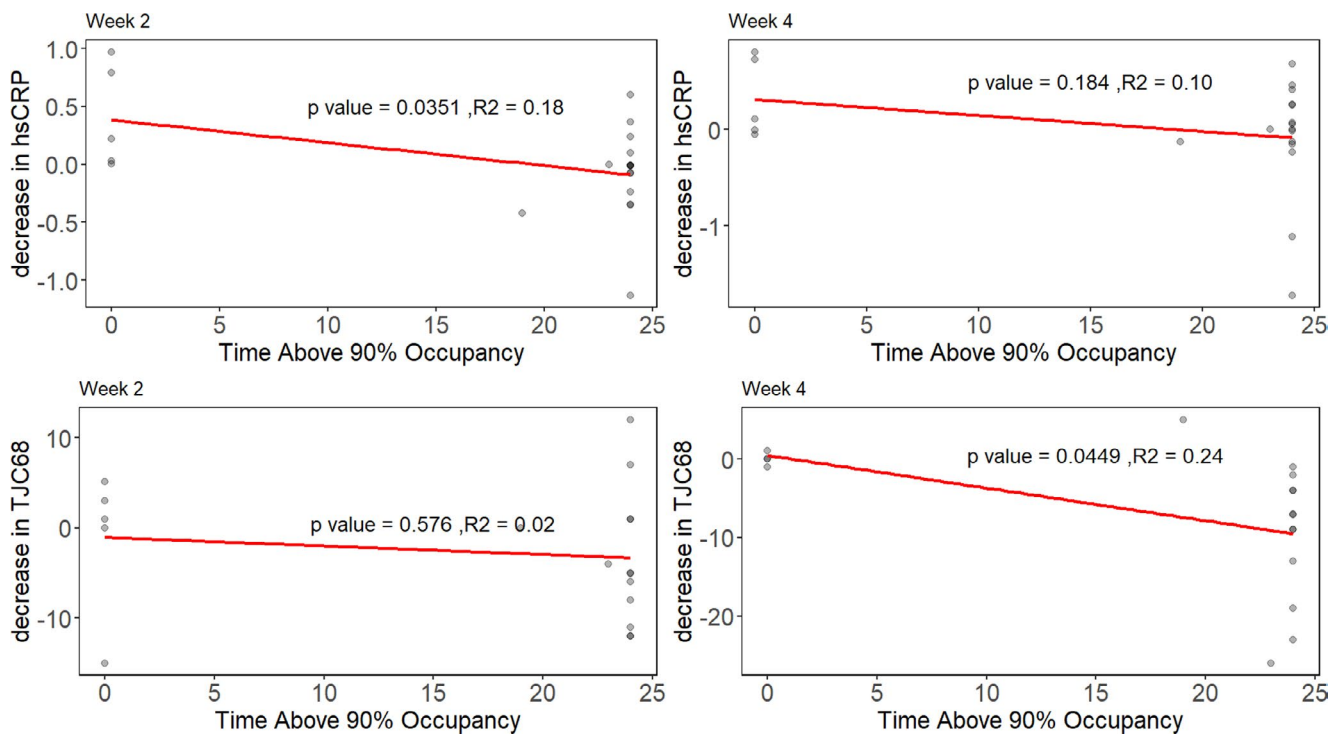


Figure 3 Exploratory linear regression for efficacy end points including hsCRP and TJC68 against time above 90% BTK occupancy. Dots show individual data points and the red line showing the regression line. hsCRP, high-sensitivity C-reactive protein; TJC68, tender joint count 68. [Colour figure can be viewed at wileyonlinelibrary.com]

statistical significance (Figure 3). The results suggest a positive trend of better efficacy with longer time over adequate BTK occupancy, however, the interpretation is limited in this safety study. A larger sample size, more stringent disease activity entry criteria, or a longer treatment duration may be required to confirm this finding.

DISCUSSION

This manuscript describes a semimechanistic PK/PD model for irreversible BTK inhibition of tirabrutinib, which was developed to support dose selection in clinical development, based on clinical PK and BTK occupancy data from two phase I studies in healthy volunteers and in subjects with RA.

The final model was assessed by different diagnostic plots, including VPC, goodness-of-fit, and NPDE (Figure 1, Figure S4–S6). In the VPC for PK and PK/PD models (Figure 1), the observed median (bold black dashed line) is aligned with the simulated median (blue solid line) and is contained within the 95% CI of the simulated median. The observed 5th and 95th percentiles (fine black dashed lines) are mostly within the 95% CI of simulated 5th and 95th percentiles. Slight overprediction of variability was observed in the terminal phase of PK with time after last dose (TALD) > 24 hours; in the early phase of fBTK, 95th percentile was slightly overpredicted before 2 hours, which may mostly result from larger fBTK variability after the first dose because fBTK would be remarkably suppressed after multiple doses of tirabrutinib. Thus, even though the model may have nuance in prediction, it may have minimal impact on the steady-state simulation within a 24-hour dosing interval after multiple dosing of tirabrutinib.

NPDE (Figure S6) shows that the central tendency in PK, fBTK, and tBTK was adequately predicted by the simulation with slight discrepancy in variability. In PK, NPDE indicates that maximum concentration (C_{max}) < 8 hours TALD may be slightly underpredicted but the difference was minimal based on PK VPC, because observed 5th, 50th, and 95th percentiles are mostly contained within its corresponding CI. For fBTK, 2.5th percentile was slightly underpredicted due to that predicted value was very close or even under the limit of detection. The 5th and 95th percentiles were moderately overpredicted at with TALD < 2 hours and after 18 hours, where BTK data were relatively sparse. We also noted that fBTK was observed to be suppressed to very low level and exhibited narrower variability at full suppression, which was reflected in the VPC for fBTK. Different IIV model (e.g., exponential, normal, Box-Cox transformation, and different IIV on different categorical covariates) and residual error model (e.g., additive, proportional, combined, and covariates on residual error) were tried some and eventually the final model was selected based on best performance to describe the variability. For tBTK, the simulation adequately captures the observed 2.5th, 50th, and 97.5th percentiles. Overall, NPDE shows that simulation is well aligned with the observed data, especially the central tendency for PK, fBTK, and tBTK. We acknowledge that 97.5th percentile of free BTK may be overpredicted and the model-based simulation could lead to relatively more conservative BTK occupancy results.

Overall, the VPC and NPDE plots show that the final PopPK model adequately predicts the central tendency of PK, fBTK, and tBTK and variability for PK and tBTK. The model can be further used for simulation of dosing regimens of interest but the simulation may lead to relatively more conservative BTK occupancy results when interpreting lower boundary in BTK occupancy variability.

The subsequent model-based simulations showed that doses of 40 mg and above are highly overlapped across the 5%–95% prediction intervals of simulated BTK occupancy, and there is a separation between ≥ 40 mg and lower doses regarding target coverage. A 40 mg dose, either q.d. or b.i.d., at steady-state can achieve 95% BTK occupancy over the dosing interval for a typical subject, and 90% of the simulated population can maintain > 90% occupancy in the peripheral blood during most of the dosing interval, which is considered adequate according to the prespecified criteria based on fenebrutinib clinical data.¹³ Based on the limited understanding of BTK turnover at site of action (e.g., synovial joint), the modeling and simulation was developed on the assumption that BTK turnover rate and BTK occupancy were similar between site of action and the peripheral blood. During the model development, BTK turnover was also estimated or fixed to different values from literature, but after all it did not have a major impact on other parameter estimation or the model fit. Overall, a total daily dose of ≥ 40 mg, either q.d. or b.i.d., was considered an adequate dose in regard to receptor occupancy for further development in inflammatory diseases, based on the PK/PD simulation.

Additional analyses were performed to explore the relationship between BTK occupancy and treatment efficacy (hsCRP and TJC68) in RA. The regressions on hsCRP at week 2 and TJC68 at week 4 show statistically significant association ($P < 0.05$) with time above 90% BTK occupancy, whereas test on hsCRP at week 4 and TJC68 at week 2 only shows a consistent trend without the statistical significance. Because study #2 was designed to evaluate the safety and PK of tirabrutinib, and active disease was not required for enrollment, efficacy data and the PD-efficacy analyses from study #2 should be interpreted with caution. A larger sample size, more stringent disease activity entry criteria, or a longer treatment duration may be required to confirm this finding.

Even though active disease was not required for enrollment in part B, study 2, baseline characteristics, including BTK and disease end points, in subjects with RA was assessed and compared with normal reference value (data not shown). This additional assessment showed that the patients with RA from part B, study 2 were different from healthy subjects with regard to baseline BTK occupancy and RA disease end points (hsCRP and TJC68) and it is therefore reasonable to evaluate the disease status covariate “RA versus healthy subjects” in the model.

In summary, a semimechanistic PK/PD model for irreversible BTK inhibition was developed for tirabrutinib, and the modeling and simulation results support a total daily dose of ≥ 40 mg, either q.d. or b.i.d., as an adequate dose in regard to receptor occupancy for further development.

SUPPORTING INFORMATION

Supplementary information accompanies this paper on the *Clinical Pharmacology & Therapeutics* website (www.cpt-journal.com).

ACKNOWLEDGMENTS

The authors thank Anita Mathias, Justin Lutz, Jeffrey Silverman, Mark Bresnik, Lianqing Zheng, John Gosink, Hao Zheng, Wanying Li, Yuanyuan Xiao, and Siddhartha Mitra for their contributions to this work. The authors also acknowledge Junjie Lu for his statistical programming effort in this work.

FUNDING

All research and modeling were funded by Gilead Sciences Inc.

CONFLICT OF INTEREST

All authors are current or former employees of Gilead Sciences, Inc., and own stock in the company. Medical writing support was provided by Impact Communication Partners (New York, NY) with financial support from Gilead Sciences, Inc.

AUTHOR CONTRIBUTION

A.M. wrote the manuscript. A.M., R.H., J.M.J., E.G., A.N.B., J.F., C.H.N., and F.M. designed the research. A.M., R.H., J.M.J., C.H.H., H.T., E.K., and C.H.N. performed the research. A.M., R.H., J.M.J., and C.H.N. analyzed the data. J.F., T.T., and H.Y. contributed new reagents/analytical tools.

© 2021 Gilead Sciences Inc. *Clinical Pharmacology & Therapeutics* published by Wiley Periodicals LLC on behalf of American Society for Clinical Pharmacology and Therapeutics

This is an open access article under the terms of the Creative Commons Attribution-NonCommercial-NoDerivs License, which permits use and distribution in any medium, provided the original work is properly cited, the use is non-commercial and no modifications or adaptations are made.

- Aoki, Y., Isselbacher, K.J. & Pillai, S. Bruton tyrosine kinase is tyrosine phosphorylated and activated in pre-B lymphocytes and receptor-ligated B cells. *Proc. Natl. Acad. Sci. USA* **91**, 10606–10609 (1994).
- Genevier, H.C. *et al.* Expression of Bruton's tyrosine kinase protein within the B cell lineage. *Eur. J. Immunol.* **24**, 3100–3105 (1994).
- Honigberg, L.A. *et al.* The Bruton tyrosine kinase inhibitor PCI-32765 blocks B-cell activation and is efficacious in models of autoimmune disease and B-cell malignancy. *Proc. Natl. Acad. Sci. USA* **107**, 13075–13080 (2010).
- Hendriks, R.W., Yuvaraj, S. & Kil, L.P. Targeting Bruton's tyrosine kinase in B cell malignancies. *Nat. Rev. Cancer* **14**, 219–232 (2014).
- Aalipour, A. & Advani, R.H. Bruton's tyrosine kinase inhibitors and their clinical potential in the treatment of B-cell malignancies: focus on ibrutinib. *Ther. Adv. Hematol.* **5**, 121–133 (2014).
- Narita, Y. *et al.* Phase I/II study of tirabrutinib, a second-generation Bruton's tyrosine kinase inhibitor, in relapsed/refractory primary central nervous system lymphoma. *Neuro. Oncol.* **23**, 122–133 (2021).
- Munakata, W. *et al.* Phase I study of tirabrutinib (ONO-4059/GS-4059) in patients with relapsed or refractory B-cell malignancies in Japan. *Cancer Sci.* **110**, 1686–1694 (2019).
- Sekiguchi, N. *et al.* A multicenter, open-label, phase II study of tirabrutinib (ONO/GS-4059) in patients with Waldenstrom's macroglobulinemia. *Cancer Sci.* **111**, 3327–3337 (2020).
- Di Paolo, J.A. *et al.* Specific Btk inhibition suppresses B cell- and myeloid cell-mediated arthritis. *Nat. Chem. Biol.* **7**, 41–50 (2011).
- Khan, W.N. Regulation of B lymphocyte development and activation by Bruton's tyrosine kinase. *Immunol. Res.* **23**, 147–156 (2001).
- Niuro, H. & Clark, E.A. Regulation of B-cell fate by antigen-receptor signals. *Nat. Rev. Immunol.* **2**, 945–956 (2002).
- Liao, C. *et al.* Selective inhibition of spleen tyrosine kinase (SYK) with a novel orally bioavailable small molecule inhibitor, R09021, impinges on various innate and adaptive immune responses: implications for SYK inhibitors in autoimmune disease therapy. *Arthritis Res. Ther.* **15**, R146 (2013).
- Cohen, S. *et al.* Fenebrutinib versus placebo or adalimumab in rheumatoid arthritis: a randomized, double-blind, phase II trial (ANDES Study). *Arthritis Rheumatol.* **9**, 1435–1446 (2020).
- Schafer, P.H. *et al.* Spebrutinib (CC-292) affects markers of B cell activation, chemotaxis, and osteoclasts in patients with rheumatoid arthritis: results from a mechanistic study. *Rheumatol. Ther.* **7**, 101–119 (2020).
- Wu, J., Zhang, M. & Liu, D. Bruton tyrosine kinase inhibitor ONO/GS-4059: from bench to bedside. *Oncotarget* **8**, 7201–7207 (2017).
- Daniilov, A.V. *et al.* Phase Ib study of tirabrutinib in combination with idelalisib or entospletinib in previously treated chronic lymphocytic leukemia. *Clin. Cancer Res.* **26**, 2810–2818 (2020).
- Morschhauser, F. *et al.* Phase 1b study of tirabrutinib in combination with idelalisib or entospletinib in previously treated B-cell lymphoma. *Leukemia* **35**, 2108–2113 (2021).
- Liclican, A. *et al.* Biochemical characterization of tirabrutinib and other irreversible inhibitors of Bruton's tyrosine kinase reveals differences in on- and off-target inhibition. *Biochim. Biophys. Acta Gen. Subj.* **1864**, 129531 (2020).
- Ariza, Y., Murata, M., Ueda, Y. & Yoshizawa, T. Bruton's tyrosine kinase (Btk) inhibitor tirabrutinib suppresses osteoclastic bone resorption. *Bone Rep.* **10**, 100201 (2019).
- Walter, H.S. *et al.* A phase 1 clinical trial of the selective BTK inhibitor ONO/GS-4059 in relapsed and refractory mature B-cell malignancies. *Blood* **127**, 411–419 (2016).
- Cockcroft, D.W. & Gault, M.H. Prediction of creatinine clearance from serum creatinine. *Nephron* **16**, 31–41 (1976).
- Yu, H. *et al.* Homogeneous BTK occupancy assay for pharmacodynamic assessment of tirabrutinib (GS-4059/ONO-4059) target engagement. *SLAS Discov.* **23**, 919–929 (2018).
- Zhang, L., Beal, S.L. & Sheiner, L.B. Simultaneous vs. sequential analysis for population PK/PD data I: best-case performance. *J. Pharmacokinet. Pharmacodyn.* **30**, 387–404 (2003).
- Beal, S.L. & Sheiner, L.B. NONMEM User's Guide (1999).
- Lindbom, L., Ribbing, J. & Jonsson, E.N. Perl-speaks-NONMEM (PsN)—a Perl module for NONMEM related programming. *Comput. Methods Programs Biomed.* **75**, 85–94 (2004).
- Lindbom, L., Pihlgren, P. & Jonsson, E.N. PsN-Toolkit—a collection of computer intensive statistical methods for non-linear mixed effect modeling using NONMEM. *Comput. Methods Programs Biomed.* **79**, 241–257 (2005).
- Ette, E.I. Stability and performance of a population pharmacokinetic model. *J. Clin. Pharmacol.* **37**, 486–495 (1997).
- Herman, A.E. *et al.* Safety, pharmacokinetics, and pharmacodynamics in healthy volunteers treated with GDC-0853, a selective reversible Bruton's tyrosine kinase inhibitor. *Clin. Pharmacol. Ther.* **103**, 1020–1028 (2018).
- Jürgensmeier, J.M. *et al.* Abstract 4082: Time- and exposure-dependent pharmacodynamic changes induced by the BTK inhibitor GS-4059 in healthy subjects. *Cancer Res.* **77**, 4082 (2017).
- Nelson, C.H. *et al.* American Society for Clinical Pharmacology and Therapeutics. *Clin. Pharmacol. Ther.* **101**, S5–S99 (2017).
- Evans, E.K. *et al.* Inhibition of Btk with CC-292 provides early pharmacodynamic assessment of activity in mice and humans. *J. Pharmacol. Exp. Ther.* **2**, 219–228 (2013).